Available online at www.jourcc.com

Journal homepage: www.JOURCC.com

Journal of Composites and Compounds

Experimental Investigation of Governing Parameters in the Electrospinning of Poly(3-hydroxybutyrate)-Starch Scaffolds: Structural Characterization

Maryam Abdollahi Asl [a], *Mohammad Mohammadalipour* [b], *Saeed Karbasi* [c]*

[a] *Tissue Engineering and Regenerative Medicine Institute, Central Tehran Branch, Islamic Azad University, Tehran 1469669191, Iran*

[b] *Department of Chemical Engineering, Isfahan University of Technology, Isfahan 84156-83111, Iran*

[c] *Department of Biomaterials and Tissue Engineering, School of Advanced Technologies in Medicine, Isfahan University of Medical Sciences, Isfahan, Iran*

ABSTRACT

In this study, for the first time, electrospinning of polyhydroxybutyrate/starch was done and optimized to produce uniform-size and bead-free nanofibers following Taguchi methodology. The main parameters such as solvent type, applied voltage, flow rate and rotating speed play an essential role in the characteristics of the nanofibrous morphologies. It found out from the main effects that the solvent type (chloroform/dimethylformamide, trifluoroacetic acid) is the most effective factor in the diameter and quality of the fibers. A scanning electron microscope assessed the structure and the average diameter of the fibers. The results indicated that all scaffolds have three-dimensional structures with interconnected porosity. The optimum levels of factors were determined as follows: 18 kV of voltage, 0.75 µL/h of flow rate, 15 cm of distance, and TFA as solvent in order to obtain the thinnest bead-free nanofibers.

Peer review under responsibility of JCC Research Group

ARTICLE INFORMATION

Article history:
Received 15 January 2022
Received in revised form 19 February 2022
Accepted 6 March 2022

Keywords:
Electrospinning
Polyhydroxybutyrate
Scaffold
Starch
Taguchi method

1. Introduction

Tissue engineering is recently being developed to supply the high demand for human tissue and organ substitutes [1]. This approach has the potential to overcome challenges in autologous and allogeneic tissue transplanting such as donor site morbidity, limited availability and adverse immune responses [2].

There are many considerable factors such as biocompatibility, controlled biodegradability, architecture, mechanical features and fabrication method in investigating the compatibility of a scaffold for tissue engineering applications [2, 3]. It has always been a challenge for tissue engineers to design and fabricate scaffolds to mimic the naturally occurring extracellular matrix (ECM) for providing an optimum cell-material and cell-cell connection through structure or chemistry [4]. Appropriate selection of biomaterials, consumed in fabricating scaffolds is very important in the final features of a scaffold. One kind of unique polymers, used in fabrication of tissue engineering scaffolds, is polyhydroxy alkanoates (PHAs) [5].

PHAs are a group of aliphatic polyesters produced by a wide variety of bacteria under specific conditions. Polyhydroxybutyrate (PHB), a tremendous group of PHAs, has become a focal research point due to its biodegradable and biocompatible characteristics [6].

Moreover, due to the valuable features of this polymer, such as good mechanical strength, dimensional stability, abrasion resistance, inherent piezoelectric properties, PHB was effectively chosen for the fabrication of tissue scaffolds [5, 6]. Piezoelectric materials can affect electrically stimulate different cell types in vitro and in vivo and play an important role in tissue regeneration [6].

In turn, PHB exhibits brittleness and surface hydrophobicity with a low degradation rate, making it less qualified to fabricate engineered scaffolds. In order to minimize the limitations mentioned above, PHB is required to be alloyed with other biomaterials to improve its mechanical features and attune other biophysical properties [7]. Researchers believe that blending PHB with natural polymers could modify its features [6, 7].

Due to their high biocompatibility, biodegradability and hydrophilicity, natural polysaccharides such as starch receive considerable attention as a natural renewable material. Starch as an abundant and inexpensive biopolymer widely employed in pharmaceutical and medical applications [8]. Starch is composed of two kinds of polysaccharides as shown in Fig. 1. Exclusively consist of linear amylose with α-(1,4) linkages (normally 20–30%) and α-(1,6) branch linkages in amylopectin (normally 70–80%); the of (1, 4)-linked α-D-glucose units and the latter is formed by (1, 6)-linked branch of the (1, 4)-linked α-D-glucose structure [9].

A combination of synthetic polymers with starch improves the biocompatibility, physical properties and degradation rate. For instance, a

* *Corresponding author: Saeed Karbasi; E-mail: karbasi@med.mui.ac.ir*

https://doi.org/10.52547/jcc.4.1.2

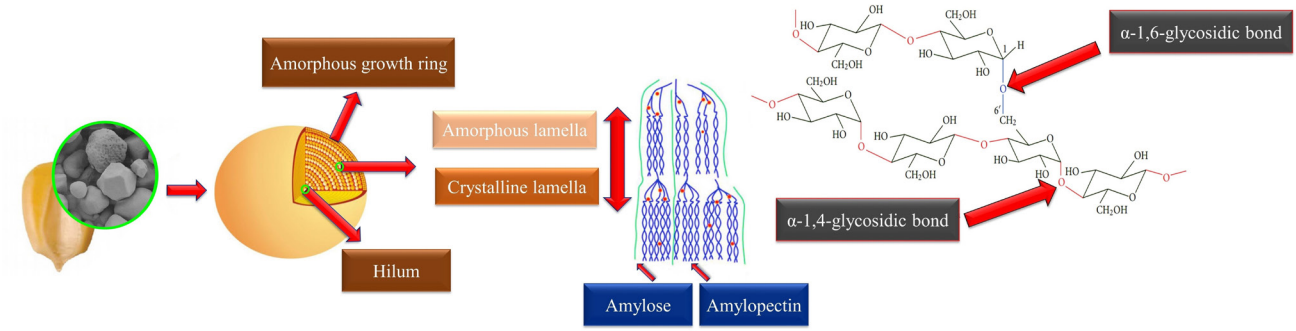

Fig. 1. Chemical structure of starch with amylose and amylopectin units.

combination of polycaprolactone (PCL) with starch increases the mechanical function, hydrophilicity and enhances cell adhesion and proliferation compared to pure PCL [10]. Sukyte et al. attempted to fabricate polyvinyl alcohol (PVA)/Starch nanofibers by electrospinning method to overcome the disadvantages of PVA such as low degradation rate and water resistant features [11]. Zhang et al. also produced poly (lactide-co-glycolide) PLGA/starch composite fibers via coaxial electrospinning technique. This study reported that hydrophilicity and degradability of scaffolds improve after adding starch to PLGA fibers [12].

Another fundamental factor in scaffolding is the fabrication technique. There are several methods to fabricate a scaffold, but electrospinning has developed as a practical method which prepares novel porosity with exclusive features [13].

In this method, high voltage is applied to the nozzle, letting the polymer solution create a cone. Then the jet forms fibers during drying and deposits them on the collector plate [11, 13].

Electrospun nanofibers can mimic the native extracellular matrix, which demonstrates a vital role for cells to migrate and proliferate in engineered scaffolds. In recent decades, the electrospinning method has attracted remarkable attention for the fabrication of nanofibers with various synthetic and natural polymers [12, 13]. Nanofibers have unique advantages in terms of high surface-to-volume ratio, combination control to achieve the required function and features, good formability, which is essential for influencing the desirable size, shape and morphology [14].

Electrospinning is a very effective method utilized to fabricate micron to submicron diameter nanofibers. Many researchers have extensively studied the fabrication of various scaffolds with both synthetic and natural polymer for regenerating damaged tissues involving bone, dentin, cartilage, collagen, liver, and skin. The development of this method aims to use tissue engineering for repair, replace and enhance the function [13, 14].

The only challenging aspect of electrospinning is the difficulty in controlling pores in scaffolds and the final structure of the interconnection and the resulting permeability [15]. In addition to the processing parameter, solution parameters such as viscosity and surface tension and their volatility and conductivity are other eminent factors that primarily affect the fluid governing rheological behavior [15, 16].

The fiber diameter distribution and morphology are dependent on the solvent type and the processing parameters. The selection of solvent is a key factor in forming a homogeneous and beadless electrospun nanofiber [17]. Generally, there are two points which need to be considered before selecting the solvent. First, the selected solvents must have polymers that are completely soluble for electrospinning process. Second, the solvent should have a moderate boiling point for appropriate volatility during electrospinning process [18, 19].

In this study, PHB and starch alloy solutions were fabricated using electrospinning method. In order to optimize the best ratio regarding the structural features, the impacts of solvent and electrospinning parameters on nanofiber features and porosity percentage were gathered and analyzed. In addition, this research presents a robust statistical Taguchi design of experiments (DOE) to systematically analyze the effects of proceeding and solution parameters on the fiber diameter. Optimum conditions were evaluated to improve the material function and yield higher productivity of electrospun scaffolds. To the best knowledge of the authors here there exist no studies have been done on the combination of PHB-starch and the optimization of their electrospinning parameters.

2. Experimental procedure

2.1. Materials

Maize starch with chemical formula $(C_6H_{10}O_5)_n$ and average molecular weight 106 g/mol, amylose: amylopectin 26:74%} was purchased from Cargill Company (C*Gel 03401), and Poly (3-hydroxybutyrate) powder (CAS 29435-48-1) with an average molecular weight 260 g/mol was purchased from Sigma–Aldrich USA. Trifluoroacetic acid (TFA) was obtained from CDH, India, and chloroform (CF) (CAS 67-66-3) and Dimethylformamide (DMF) (CAS 68-12-2) were supplied from Merck Company of Germany for the fabrication of scaffolds.

2.2. Fabrication of electrospun scaffolds

In order to compare the effect of the solvent on characteristics of fibers, polymeric solutions were prepared by dissolving 9% wt. PHB in chloroform/DMF and TFA. The PHB powder was dissolved in TFA by magnetic stirring for 1h at 50 °C. Then, 10 wt. %. of starch was added to the PHB solution and was stirred for 2 h. For samples with chloroform/DMF, solvent (8:2 v/v) at first PHB was dissolved in chloroform at 60 °C for 2 h. After that, DMF and 10 wt. %. of starch were added to the solution and stirred for 1h at 40 °C. A 1cc syringe, including a 23 gauge medical-used needle, was loaded with the prepared solution and placed on the syringe pump device. All nanofiber samples were collected on the aluminum foil and the rundle collector was rotated at range 325 rpm.

2.3. Processing parameters

Electrospinning parameters affecting the fiber features are the distance between the needle tip and collector, feeding rate of the polymer solution and applied voltage. This specific polymer/solvent system's applied voltage was determined with three distinct values: 12, 15, and 18 kV. In addition, flow rate is one of the key parameters in adjusting fiber diameter and its distribution, primary droplets shape, maintenance of Taylor cone and deposition area. It is believed that optimal feeding rates are assigned in causing the solvent to have adequate time for evaporation [20, 21]. Therefore, optimization injection ratio was determined at 0.5,

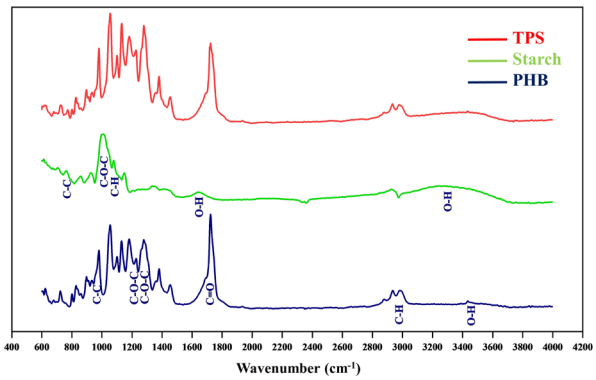

Fig. 2. ATR-FTIR spectrum of PHB and PHB-starch (TPS) scaffolds.

0.75, 1mL/h. The nozzle collector distance was fixed at 15 cm.

2.4. Experiment Design

Taguchi method, as a simple statistical study, has three main steps: 1) select factors and their different levels to design the experiment, 2) conduct the ideal design experiment and 3) evaluate the obtained results.

According to this study, Taguchi method makes it possible to investigate the effect of different factors on project results [17]. In this study, based on the literature review and previous research experiences, the distance between the tip of needle and collector plate was fixed at 15 (cm), which was also confirmed by an optical microscope [20-22]. Then, the injection rate (mL/h) and applied voltage with three different levels (kV) were considered the most important factors affecting electrospinning. The standard L9 (3*2) design based on Taguchi algorithm was used, and designed experiments were conducted according to Table 1. T1-T9 and ChD1-ChD9 refer to PHB-starch scaffolds prepared by TFA and chloroform/DMF, respectively.

2.5. Structural characteristics

2.5.1. FTIR- ATR characterization

Attenuated Total Reflectance-Fourier Transform Infrared (FTIR-ATR, Bruker, Tensor 27/Germany) was applied to evaluate the chemical bonding between the PHB and starch. The spectra of FTIR-ATR were recorded in wavenumber within 400 and 4000 cm^{-1} range at room temperature. FTIR-ATR was conducted for PHB, starch and PHB-starch electrospun scaffolds, and analysis was carried out with standard Microcal Origin software (Northampton, MA).

Table 1.
Standard L9 (3*2) design based on Taguchi Algorithm, by MiniTab19 software

Sample No.	Codes	Voltage (kV)	Rate (mL/h)
1	T1	12	0.5
2	T2	15	0.5
3	T3	18	0.5
4	T4	12	0.75
5	T5	15	0.75
6	T6	18	0.75
7	T7	12	1
8	T8	15	1
9	T9	18	1
10	ChD1	12	0.5
11	ChD2	15	0.5
12	ChD3	18	0.5
13	ChD4	12	0.75
14	ChD5	15	0.75
15	ChD6	18	0.75
16	ChD7	12	1
17	ChD8	15	1
18	ChD9	18	1

***T1-T9 (Prepared by TFA) and ChD1-ChD9 (Prepared by chloroform/DMF)

2.5.2 Evaluation of scaffold morphology

The morphology, porosity and integrity of the fibers were evaluated by scanning electron microscope (SEM, SERONTECHNOLOGIES, AIS2100/South Korea). The surfaces of the electrospun scaffolds were sputter-coated with gold samples by a sputter-coating machine (Emitech SC7620 Sputter Coater; Quorum Technologies/UK) for 15 minutes before examination [23]. All the images had the same magnification and were taken to facilitate further image analysis.

The average fiber diameter was calculated by measuring the diameter of 100 single fibers from 6 different SEM images using image J analysis software (Image J 1.51, Java 1.6.0_24 (64-bit), national institutes of health; USA) for each group .

The porosity of three surface layers was calculated with five SEM images by MATLAB (R2016a) software program [24]. Porosity is defined as the ratio of pore spaces to the total volume of scaffold, which is calculated from Eq (1).

$$P = (V_o/V_T) \quad (1)$$

Where P is the porosity of the scaffold, V_o is regarded as the measure of open cavities and V_T represents the total volume.

2.6. Statistical analysis

All the experiments were performed with n = 3 and statistical calculations of the results were reported as mean ± SD at a statistical significance level of $P<0.05$.

3. Results and discussions

3.1. ATR-FTIR assessment

ATR-FTIR spectroscopy test in order to accentuate the bands was done to characterize the functional groups of polymers and solvent effect in this study. ATR spectra of PHB, starch and TPS scaffolds (scaffolds prepared by TFA solvent) are presented in Fig. 2. The prominent feature of PHB scaffold at 979 cm^{-1}, 1180 cm^{-1}, 1228 cm^{-1}, 1276 cm^{-1}, 1722 cm^{-1} and the region of 2970-3010 cm^{-1} is related to the C-C stretch, C-O-C asymmetric stretch of the amorphous phase, C-O-C stretch, symmetric C-O-C stretch of crystalline phase, stretch absorption of carbonyl group, and C-H carboxyl group, respectively [4].

For starch powder, the spectrum showed its characteristic functional groups. The peaks at 814 cm^{-1} and 734 cm^{-1} can be related to the C-H, CH_2 deformation and C-C stretching vibration, respectively. The peaks at 957 cm^{-1} and 1003 cm^{-1} are denoted to the skeletal and stretching vibration of the C-O-C α-1-4 glycosidic bond, respectively. The peak at 1131 cm^{-1} is the C-O-C symmetric stretching of the cyclic ether group, while that at 1080 cm^{-1} belongs to C-H bending vibrations region. The band at 1647 cm^{-1} is the bending vibration of the hydroxyl group of water absorbed in the amorphous regions of starch, and the peak at 2925 cm^{-1} is the -CH_2- stretching vibration. Eventually, the broad peak at 3100-3500 cm^{-1} can correspond to water directly bound by hydrogen bonding to the hydroxyl groups of the double helices of starch. The visible peak at 3500 cm^{-1} indicates that water molecules are indirectly bound to the hydroxyl groups via other water molecules [9].

Although there are apparent similarities in obtained spectra due to the low weight percentage of starch, by adding starch, abundant hydrox-

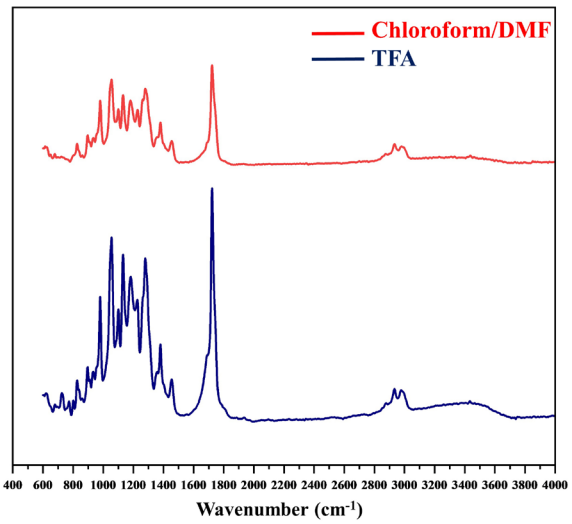

Fig. 3. ATR-FTIR spectrum of PHB-starch scaffolds prepared by TFA (T) and Chloroform/DMF (ChD).

yl groups (broad peak around 3300) make a significant difference in ATR spectra of TPS compared to the pure PHB. The mentioned change is evident at around 3400 cm^{-1}. In Fig. 2, TPS is related to the hydroxyl groups of starch [7].

In addition, the center region of the hydroxyl group in TPS scaffolds shifts to a higher wavenumber in comparison to the pure starch, indicating the formation of intermolecular hydrogen bonds between PHB and starch. Moreover, it is obvious that the peaks in the carbonyl region have weak broad adsorption compared to those in TPS scaffolds. These results illustrate that the hydrogen bonding occurred between the hydroxyl groups on the glucose ring in the starch chains and the carbonyl groups in the PHB participate in the intermolecular interactions. The same trend is observed in [20, 21].

Fig. 3 shows the difference between ATR spectrum of the samples prepared by TFA and ChD solvents system at a constant concentration of PHB and starch. Generally, due to the high ability of TFA and fluorine to create a strong hydrogen-bonding network, as the order of the chains increases, it is likely that the intensity of the peaks is increased accordingly. As it can be seen in Fig. 3, the entire signal intensity appears to be lower in the ChD sample. Therefore, it can be inferred that TFA provides a better solvation effect and it is more appropriate [21]. In this regard, Fig. 5 (SEM investigation section) also indicates the weakness of ChD solvent system to provide a perfectly uniform network.

3.2. Evaluation of scaffold morphology based on solvents

3.2.1. TFA solvent system

SEM images of PHB-starch scaffolds prepared by TFA (T1-T9) solvent system in Table1 are shown in Fig. 4.

SEM images of fibers surface in different scales showed that the obtained fibers were uniform, smooth and bead-free. The morphology of uniform fibers in scaffold provides a high surface area and interconnected holes to improve the exchange of nutrients, oxygen and cell proliferation potential [22].

3.2.2. Chloroform/DMF solvent system

SEM images of scaffolds fabricated with chloroform/DMF solvent are shown in Fig. 5. It is obvious that heterogeneity in fiber diameter and agglomeration with a rough surface are obtained. This rough surface was probably because of the high rate of chloroform evaporation, which caused the outer surface of the fibers to dry, and the first evaporation of solvent from inside the fibers caused the skin to collapse [23]. It can be found that uniform, smooth and bead-free nanofibers can be obtained by proper selection of solvent type under each process condition.

Table 1 shows the average diameter and standard deviation (SD) of the obtained electrospun PHB-starch fibers. A wide range of fibers diameters from 312 to 1450 nm are produced through different solvent system and parameter selections.

It should be noticed that the standard deviation of fibers fabricated by chloroform/DMF solvent system is very large (for instance, samples 4, 5, 9, and 7). It means that in these samples, the fibers are inhomogeneous. On the other hand, the standard deviation of the fibers fabricated by TFA solvent system was small and homogeneous.

The fiber diameter is closely related to the porosity percentage. Operational scaffolds in tissue engineering possess an optimum fiber diameter and porosity. Sufficient porosity of scaffolds is a fundamental factor for providing a microenvironment to promote cell infiltration, growth, nutrient diffusion and vascularisation during tissue regeneration [24].

The results of all samples are shown in Table 3. The porosity of electrospun fibers is generally high, which could be appropriate for tissue engineering. The porosity percentage in the first layer of scaffolds was approximately measured in the range of 75 to 86 %.

The porosity of the 2nd and 3rd layers indicated that there is interconnectivity between pores. These features could have adequate space to circulate for cell development [25].

Based on the result, increase in the applied voltage and decrease in the flow rate caused fiber diameters to be reduced. Subsequently, decrease in fiber diameters resulted in higher porosity percentage. However, there was no significant difference between porosity percentages of layers in both types of solvents ($p > 0.05$).

Jabur et al. studied the effect of flow rate on some physical properties of PVA electrospun scaffold. They concluded that by decreasing the flow rate, the porosity percentage will be increased due to the decrease in the fiber diameter [26].

In addition, Mahalingam et al. investigated the solubility–spinnability of polyethylene terephthalate (PET) for various solvents. This research implied that the TFA solvent could lead to the continuous defect-free structure of nanofiber [27].

Table 2.
Mean fiber diameter of electrospun scaffolds.

Codes	Nanofiber Diameter (nm)	C.V.	SD
T1	770.72	0.608	29.24
T2	517.04	0.345	48.60
T3	468.29	0.183	55.77
T4	433.95	0.283	22.74
T5	181.78	0.244	86.57
T6	336.97	0.366	23.50
T7	490.34	0.550	24.46
T8	400.60	0.310	24.36
T9	412.06	0.508	58.05
ChD1	1130.73	0.635	141.32
ChD2	584.17	0.770	145.04
ChD3	578.33	0.618	135.35
ChD4	1371.37	1.481	120.16
ChD5	870.65	0.820	94.04
ChD6	683.08	0.389	126.68
ChD7	1450.99	1.439	120.28
ChD8	1281.74	0.199	125.03
ChD9	1231.10	0.769	127.43

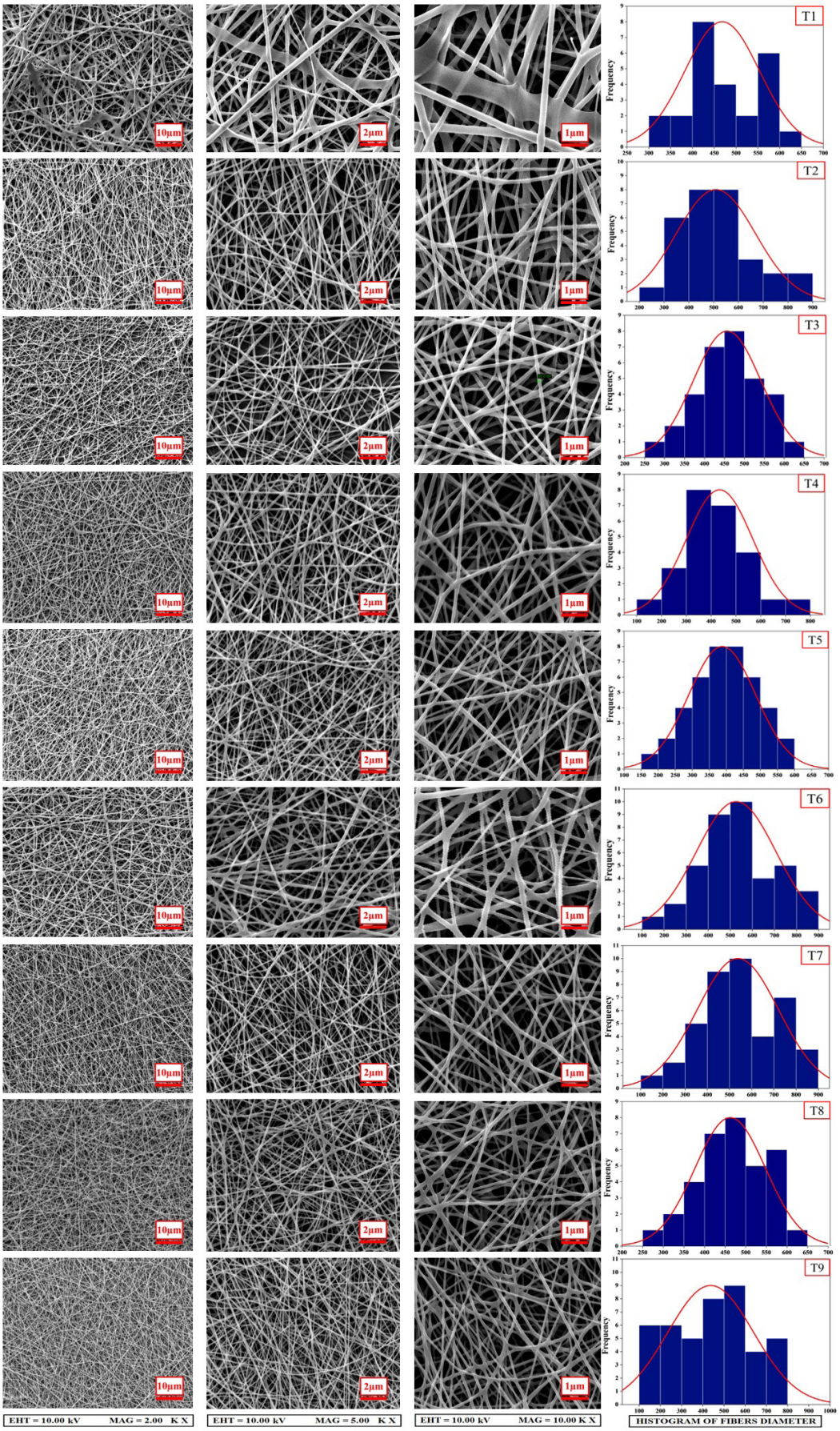

Fig. 4. SEM images at 1000, 5000 and 10,000 magnifications and histograms illustrating the diameter distribution of PHB-starch scaffolds prepared by TFA (T1-T9).

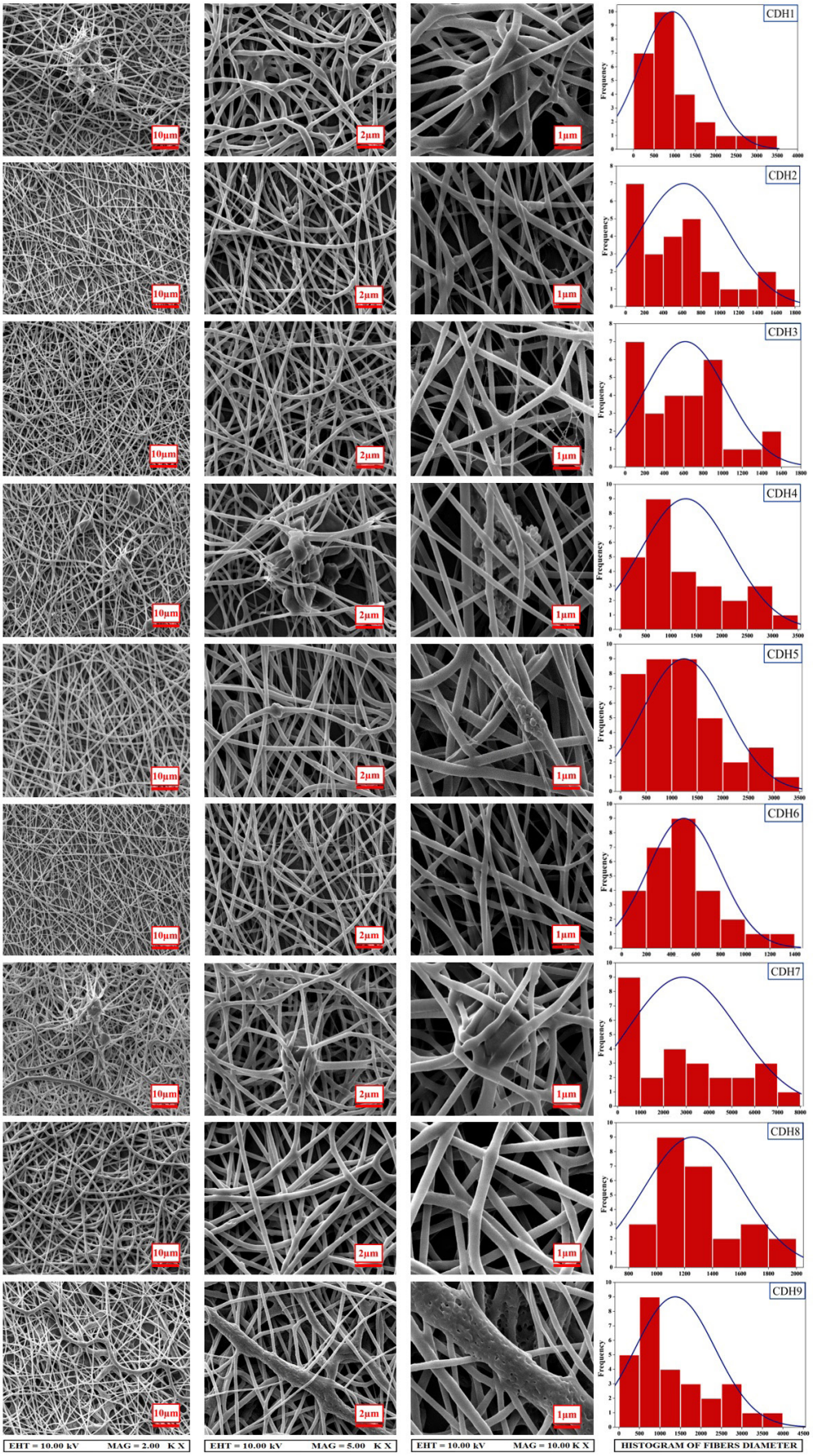

Fig. 5. SEM images at 1000, 5000 and 10,000 magnifications and histograms illustrating the diameter distribution of PHB-starch scaffolds prepared by Chloroform/DMF solvent system (ChD1-ChD9).

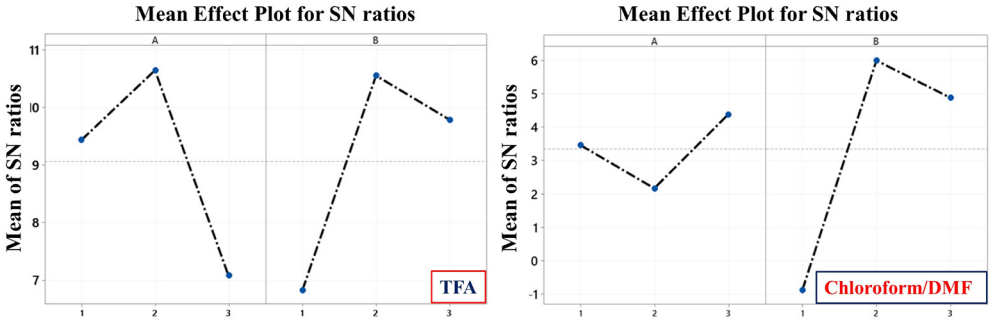

Fig. 6. The S/N ratios plot for C.V. of fibers diameter; prepared by (a) TFA, (b) Chloroform/DMF.

3.3. Evaluation of scaffold morphology based on processing parameters

3.3.1. Applied voltage

The applied voltage is a crucial element in electrospinning process because it can the charged jets ejected from Taylor cone to occur. Generally, instability and stretching of the jet increase with applied voltage and lead to a decrease in nanofiber diameters [28].

In electrospinning experiments, higher values of applied voltage can increase the electrostatic repulsive force on the charged jet and decrease the fiber diameter; therefore, the solvent evaporates quickly and no beads are formed [27, 28]. Nevertheless, some polymers exhibit different behaviors; for example, high voltage has no effect on fiber diameter for electrospinning of polyethylene oxide [29].

Table 1 shows the condition of this experiment with different applied voltages. Electrospinning jet started ejecting from 10 kV, but the electrostatic forces were not strong enough to continue this process at the tip of the needle. Afterwards, the electrospinning started from 12 kV and the stable jet continued electrospinning constantly. It is clear that the average fiber diameter in scaffolds prepared by TFA (T1-T9) solvent is less than chloroform/DMF solvent [30, 31]. However, the effects of applied voltage on fiber diameter should be considered with other parameters, particularly, with the flow rate and distance between the metallic needle of the syringe and the grounded collector.

Table 3.
Porosity percentage of the scaffolds in three layers based on MATLAB image processing

Codes	Porosity of first layer	Porosity of second layer	Porosity of third layer
T1	77± 0.8%	63± 0.9%	50± 0.4%
T2	77 ± 0.4%	65 ± 0.7%	53 ± 0.3%
T3	80 ± 0.4%	69 ± 0.5%	54 ± 0.7%
T4	83 ± 0.5%	70 ± 0.9%	56 ± 0.5%
T5	81 ± 0.8%	68 ± 0.5%	53 ± 0.8%
T6	80 ± 0.3%	67± 0.9%	51 ± 0.3%
T7	81± 0.4%	68 ± 0.7%	55± 0.4%
T8	83 ± 0.2%	70± 0.5%	53 ± 0.8%
T9	86± 0.8%	75 ± 0.7%	59 ± 0.7%
ChD1	82 ± 1.5%	72 ± 0.9%	56 ± 1.4%
ChD2	83 ± 1.2%	70 ± 1.1%	51± 0.9%
ChD3	86 ± 0.8%	77 ± 1.2%	54 ± 1.2%
ChD4	80 ± 1.4%	67± 2.1%	50 ± 1.2%
ChD5	81± 1.2%	69± 1.5%	58± 1.6%
ChD6	75± 1.4%	62± 1.2%	50± 1.2%
ChD7	81± 1.2%	71± 1.8%	55± 2.1%
ChD8	83± 0.8%	68± 0.9%	51± 1.2%
ChD9	79± 2.2%	60± 1.9%	42± 2.2%

3.3.2. Flow rate

Flow rate is another considerable parameter in controlling fiber diameter and its homogeneity. It is believed that larger droplets are formed at high flow rates, which increases the average fiber diameters due to the short drying time to reach the collector plate and low stretching forces [32].

In this study, based on observations obtained from the optical microscope, flow rates were selected in the range of 0.5, 0.75,1 mL/h. The diameters of the electrospun nanofibers increase, as the flow rates decrease. The reason is that low feeding rate is favorable for the evaporation of solvent, which results in the formation of solid nanofiber. Ideally, flow rate must match with evaporation rate from the tip of the needle. According to Zhenyu et al., lower flow rates are more favorable. High flow rates lead to large diameter fibers with a bead because the solvent evaporates to reach the collector over time [32]. The same trend is reported in [29-32] .

3.4. Designed results based on Taguchi method

Eventually, the effect of each parameter on the uniformity of fibers diameter, which is a much more important feature than the fiber size, was evaluated by Minitab19 software. The coefficient variation (C.V.), as an appropriate criterion of distribution of fibers diameter, was calculated from equation 1:

$$C.V. = \frac{\sigma}{\mu} \quad (1)$$

Where σ and μ are standard deviation (SD) and average fiber diameter, respectively. The actual impact of each factor and the optimal condition can be obtained by the S/N ratio, a reliable response that has the least variance. Therefore, this ratio for C.V. of the fibers diameter was based on “smaller is better” type and was calculated from equation 2:

$$S/N = -10 \log \text{mean standard deviation (MSD)} \quad (2)$$
$$MSD = (y_1^2 + y_2^2 + \ldots + y_n^2) / n$$

In this equation, n and y indicate the numbers of observations and the experimental data, respectively [33, 34]. Fig. 6 shows the S/N ratio of various levels of factors and distribution of fibers diameter. As expected, S/N ratios plot indicates these factors, which significantly affect the results. In the case of TFA solvent, the second level of factors gave the best output. In other words, based on S/N ratios plot, voltage and injection rate with values of 15 kV and 0.75 mL/h are the optimal values of factors to achieve uniform fibers.

In the case of secondary solvent system, although SEM images show that the fibers are not as clean as the fibers obtained by TFA and this solvent system is not very practical, the best levels of voltage and injection rate for electrospinning of PHB-starch solution are 15kV and 1mL/h,

respectively.

Taguchi experiment results indicate that the first level of voltages was rejected in both cases since electrostatic forces could not stretch the solution at low voltages. Increasing the voltage makes the fibers more uniform due to the solution drawn from the tip of the needle [35]. Fig. 6 shows that the second and third levels of voltages are significantly superior to the first one. The feeding rate enhancement similarly increases the jet velocity. However, if it is not properly controlled, it could have adverse effects on the uniformity of fibers diameter distribution and morphology [35].

To prevent defects, feeding rate increment should be enough to provide sufficient time for the complete evaporation of the solvent. Although the S/N difference in chloroform/DMF system is less than a unit, in the case of TFA solvent, Fig. 6 shows that 0.75 mL/h is significantly preferable.

4. Conclusions

The electrospinning method can provide incomparable operational simplicity to achieve tremendous potential in specific tissue engineering applications by mimicking native ECM. In this study, high porosity structure of PHB-starch was fabricated using electrospinning method. As one the most notable techniques of experimental design, Taguchi method was employed to optimize the major electrospinning factors for two types of solvents to achieve the smallest nanofiber diameter. The fiber distribution in scaffolds prepared by TFA (T1-T9) solvent is uniform, compared to those prepared by chloroform/DMF (ChD1-ChD9). ATR-FTIR indicated that the presence of starch and the formation of the strong hydrogen bonding between PHB and starch. Conclusively, the results revealed that the TFA solvent is the best solvent to dissolve PHB-starch polymers for alloying applications. As a result, PHB-starch scaffold provides a beneficial method for tissue regeneration. In addition, other studies including structural, physical, mechanical and biological studies are also underway on this combination.

Acknowledgement

We would like to thank Isfahan University of Medical Sciences and the Department of Biomaterials and Tissue Engineering (School of Advanced Technology in Medicine, Isfahan University of Medical Sciences, Isfahan, Iran) for providing the means for this experiment.

REFERENCES

[1] P.K. Chandra, S. Soker, A. Atala, Chapter 1 - Tissue engineering: current status and future perspectives, in: R. Lanza, R. Langer, J.P. Vacanti, A. Atala (Eds.), Principles of Tissue Engineering (Fifth Edition), Academic Press2020, pp. 1-35.

[2] M.A. asl, H. Ghomi, Fabrication of highly porous merwinite scaffold using the space holder method, International Journal of Materials Research 111(9) (2020) 711-718.

[3] S.S. Patil, R.D.K. Misra, The significance of macromolecular architecture in governing structure-property relationship for biomaterial applications: an overview, Materials Technology 33(5) (2018) 364-386.

[4] M.R. Foroughi, S. Karbasi, M. Khoroushi, A.A. Khademi, Polyhydroxybutyrate/chitosan/bioglass nanocomposite as a novel electrospun scaffold: fabrication and characterization, Journal of Porous Materials 24(6) (2017) 1447-1460.

[5] Z. Mohammadalizadeh, S. Karbasi, S. Arasteh, Physical, mechanical and biological evaluation of poly (3-hydroxybutyrate)-chitosan/MWNTs as a novel electrospun scaffold for cartilage tissue engineering applications, Polymer-Plastics Technology and Materials 59(4) (2020) 417-429.

[6] D. Sadeghi, S. Karbasi, S. Razavi, S. Mohammadi, M.A. Shokrgozar, S. Bonakdar, Electrospun poly(hydroxybutyrate)/chitosan blend fibrous scaffolds for cartilage tissue engineering, Journal of Applied Polymer Science 133(47) (2016).

[7] P. Naderi, M. Zarei, S. Karbasi, H. Salehi, Evaluation of the effects of keratin on physical, mechanical and biological properties of poly (3-hydroxybutyrate) electrospun scaffold: Potential application in bone tissue engineering, European Polymer Journal 124 (2020) 109502.

[8] J. Su, L. Chen, L. Li, Characterization of polycaprolactone and starch blends for potential application within the biomaterials field, African Journal of Biotechnology 11(3) (2012) 694-701.

[9] A. Shafqat, A. Tahir, A. Mahmood, A.B. Tabinda, A. Yasar, A. Pugazhendhi, A review on environmental significance carbon foot prints of starch based bio-plastic: A substitute of conventional plastics, Biocatalysis and Agricultural Biotechnology 27 (2020) 101540.

[10] M.E. Gomes, H.S. Azevedo, A.R. Moreira, V. Ellä, M. Kellomäki, R.L. Reis, Starch–poly(ε-caprolactone) and starch–poly(lactic acid) fibre-mesh scaffolds for bone tissue engineering applications: structure, mechanical properties and degradation behaviour, Journal of Tissue Engineering and Regenerative Medicine 2(5) (2008) 243-252.

[11] J. Sukyte, E. Adomaviciute, R. Milasius, J. Bendoraitiene, P.P. Danilovas, Formation of poly (vinyl alcohol)/cationic starch blend nanofibres via the electrospinning technique: The influence of different factors, Fibres & Textiles in Eastern Europe (2012).

[12] H.B. Zhang, M. Zhu, R.Q. You, Modified Biopolymer Scaffolds by Co-Axial Electrospinning, Advanced Materials Research 160-162 (2011) 1062-1066.

[13] T. Wu, M. Ding, C. Shi, Y. Qiao, P. Wang, R. Qiao, X. Wang, J. Zhong, Resorbable polymer electrospun nanofibers: History, shapes and application for tissue engineering, Chinese Chemical Letters 31(3) (2020) 617-625.

[14] V. Sgarminato, C. Tonda-Turo, G. Ciardelli, Reviewing recently developed technologies to direct cell activity through the control of pore size: From the macro- to the nanoscale, Journal of Biomedical Materials Research Part B: Applied Biomaterials 108(4) (2020) 1176-1185.

[15] L. Kong, G.R. Ziegler, Quantitative relationship between electrospinning parameters and starch fiber diameter, Carbohydrate Polymers 92(2) (2013) 1416-1422.

[16] A.H. Tehrani, A. Zadhoush, S. Karbasi, S.N. Khorasani, Experimental investigation of the governing parameters in the electrospinning of poly(3-hydroxybutyrate) scaffolds: Structural characteristics of the pores, Journal of Applied Polymer Science 118(5) (2010) 2682-2689.

[17] V. Varkey, E. Tomlal Jose, U.S. Sajeev, Electrospinning technique for the fabrication of poly(styrene-co-methyl methacrylate) nanofibers and the effect of fiber diameter on UV–Visible absorption and thermal properties, Materials Today: Proceedings 33 (2020) 2077-2081.

[18] L. Wannatong, A. Sirivat, P. Supaphol, Effects of solvents on electrospun polymeric fibers: preliminary study on polystyrene, Polymer International 53(11) (2004) 1851-1859.

[19] G. Barouti, C.G. Jaffredo, S.M. Guillaume, Advances in drug delivery systems based on synthetic poly(hydroxybutyrate) (co)polymers, Progress in Polymer Science 73 (2017) 1-31.

[20] E.B. Toloue, S. Karbasi, H. Salehi, M. Rafienia, Potential of an electrospun composite scaffold of poly (3-hydroxybutyrate)-chitosan/alumina nanowires in bone tissue engineering applications, Materials Science and Engineering: C 99 (2019) 1075-1091.

[21] F. Amini, D. Semnani, S. Karbasi, S.N. Banitaba, A novel bilayer drug-loaded wound dressing of PVDF and PHB/Chitosan nanofibers applicable for post-surgical ulcers, International Journal of Polymeric Materials and Polymeric Biomaterials 68(13) (2019) 772-777.

[22] T. Yao, H. Chen, M.B. Baker, L. Moroni, Effects of Fiber Alignment and Coculture with Endothelial Cells on Osteogenic Differentiation of Mesenchymal Stromal Cells, Tissue Engineering Part C: Methods 26(1) (2019) 11-22.

[23] S. Tungprapa, T. Puangparn, M. Weerasombut, I. Jangchud, P. Fakum, S. Semongkhol, C. Meechaisue, P. Supaphol, Electrospun cellulose acetate fibers: effect of solvent system on morphology and fiber diameter, Cellulose 14(6) (2007) 563-575.

[24] A.P. Kishan, E.M. Cosgriff-Hernandez, Recent advancements in electrospinning design for tissue engineering applications: A review, Journal of Biomedical Materials Research Part A 105(10) (2017) 2892-2905.

[25] A. Timnak, J.A. Gerstenhaber, K. Dong, Y.-e. Har-el, P.I. Lelkes, Gradient porous fibrous scaffolds: a novel approach to improving cell penetration in electrospun scaffolds, Biomedical Materials 13(6) (2018) 065010.

[26] A.R. Jabur, M.A. Najim, S.A.A. Al- Rahman, Study the effect of flow rate on some physical properties of different polymeric solutions, Journal of Physics: Conference Series 1003 (2018) 012069.

[27] S. Mahalingam, B.T. Raimi-Abraham, D.Q.M. Craig, M. Edirisinghe, Solubility–spinnability map and model for the preparation of fibres of polyethylene (terephthalate) using gyration and pressure, Chemical Engineering Journal 280 (2015) 344-353.

[28] A. Haider, S. Haider, I.-K. Kang, A comprehensive review summarizing the

effect of electrospinning parameters and potential applications of nanofibers in biomedical and biotechnology, Arabian Journal of Chemistry 11(8) (2018) 1165-1188.
[29] N. Bhardwaj, S.C. Kundu, Electrospinning: A fascinating fiber fabrication technique, Biotechnology Advances 28(3) (2010) 325-347.
[30] H.H. Kim, M.J. Kim, S.J. Ryu, C.S. Ki, Y.H. Park, Effect of fiber diameter on surface morphology, mechanical property, and cell behavior of electrospun poly(ε-caprolactone) mat, Fibers and Polymers 17(7) (2016) 1033-1042.
[31] C. Viezzer, M.M.d.C. Forte, F.A. Berutti, A.K. Alves, C.P. Bergmann, Effect of electrospun phb and hap-phb composite scaffolds characteristics on mesenchymal stem cell growth viability, MOJ Applied bionics and biomechanics [recurso eletrônico]. Edmond. vol. 1, no. 6 (2017), art. 00035, 8 p. (2017).
[32] Z. Li, C. Wang, Effects of Working Parameters on Electrospinning, in: Z. Li, C. Wang (Eds.), One-Dimensional nanostructures: Electrospinning Technique and Unique Nanofibers, Springer Berlin Heidelberg, Berlin, Heidelberg, 2013, pp. 15-28.
[33] H.-W. Chen, M.-F. Lin, Characterization, Biocompatibility, and Optimization of Electrospun SF/PCL/CS Composite Nanofibers, Polymers 12(7) (2020) 1439.
[34] C. Zandén, Functional Fiber Based Materials for Microsystem Applications, Chalmers Tekniska Hogskola (Sweden)2014.
[35] H.S. SalehHudin, E.N. Mohamad, W.N.L. Mahadi, A. Muhammad Afifi, Multiple-jet electrospinning methods for nanofiber processing: A review, Materials and Manufacturing Processes 33(5) (2018) 479-498.